

Chemical pressure in $\text{SmNiC}_{2-x}\text{B}_x$ compounds: evidence of a quantum critical behavior

This content has been downloaded from IOPscience. Please scroll down to see the full text.

2014 J. Phys.: Condens. Matter 26 455602

(<http://iopscience.iop.org/0953-8984/26/45/455602>)

View [the table of contents for this issue](#), or go to the [journal homepage](#) for more

Download details:

IP Address: 132.248.12.211

This content was downloaded on 23/01/2015 at 19:00

Please note that [terms and conditions apply](#).

Chemical pressure in $\text{SmNiC}_{2-x}\text{B}_x$ compounds: evidence of a quantum critical behavior

F Morales, L F Mendivil and R Escamilla

Instituto de Investigaciones en Materiales, Universidad Nacional Autónoma de México, 04510 México DF, Mexico

E-mail: fmleal@unam.mx

Received 2 August 2014, revised 8 September 2014

Accepted for publication 15 September 2014

Published 16 October 2014

Abstract

We studied the effect of carbon substituted by boron on polycrystalline samples of SmNiC_2 in the B content range $0 \leq x \leq 0.200$. The structural parameters were determined from x-ray measurements by Rietveld analysis. The structural analysis shows that the cell volume increases as the B content increases indicating that the substitution produces an internal pressure. The samples were studied by resistance as a function of temperature from room temperature down to 2 K. The transition temperature of the charge density wave, $T_{\text{CDW}} = 148$ K, decreases with an increment of B until the transition vanishes in the resistance measurements. At the same time, the ferromagnetic transition temperature changes showing a tiny dome with the B content, with a maximum transition temperature of ~ 23.1 K. In addition, the resistance behaviour above the charge density wave is linear in temperature and this behaviour persists until the charge density wave disappears, suggesting that the system is a non-Fermi liquid. The resulting temperature—boron content phase—diagram indicates a quantum critical behaviour.

Keywords: charge density wave, ferromagnetism, chemical pressure, quantum critical point, non-Fermi liquid

(Some figures may appear in colour only in the online journal)

1. Introduction

Ternary RNiC_2 compounds ($R = \text{Y}$ or rare-earth) crystallize in an orthorhombic CeNiC_2 type structure and show interesting physical properties, such as, charge density waves (CDW), below a characteristic temperature T_{CDW} , with values between 100 K and above room temperature. At low temperatures these compounds show magnetic order, mainly of the antiferromagnetic type. The magnetic behaviour originates from the rare-earth element, the Ni magnetic contribution is negligible [1, 2]. LaNiC_2 and SmNiC_2 show different behaviours at low temperature, LaNiC_2 shows superconductivity below 2.7 K [3, 4] and SmNiC_2 shows a ferromagnetic (FM) state below 17.5 K [1].

Current literature has shown a renewed interest in SmNiC_2 because of the presence of a CDW state below 148 K, FM behaviour below a transition temperature $T_{\text{C}} = 17.5$ K,

and the relation between both processes. The CDW is incommensurate and is associated to the formation of Ni dimers along the a crystallographic axes [5]. The CDW was identified by x-ray scattering experiments where satellite peaks are observed below 148 K, and disappear when the FM state sets below 17.5 K [6]. However, the orthorhombic lattice structure persists until 9 K [5]. The CDW can be identified by measurements of resistance R as a function of temperature T , when $R(T)$ shows a metal-insulator transition. Other systems, such as NbSe_3 , show a maximum $R(T)$ below the T_{CDW} , then at lower temperatures $R(T)$ decreases again [7–9].

The application of high pressure on materials provides information about the changes on the crystal structure and the subsequent effects on its phononic and electronic properties [9–12]. High pressure experiments on SmNiC_2 showed that the CDW transition temperature increases up to 279.3 K with 5.5 GPa [13]. In addition, a second CDW is observed

at pressures of 2.2 GPa. Regarding the FM transition temperature, it decreases down to 5 K with a pressure of 4 GPa. The temperature–pressure phase diagram of SmNiC_2 shows a complex behaviour, in addition to ferromagnetism, and three more regions with magnetic order above 2.14 GPa exist.

An equivalent way to study the effects of pressure is to study the chemical pressure. Chemical pressure is produced by the substitution of one element of the compound, in order to reach a cell volume change. The volume could increase or decrease depending on the difference in atom size. As an example, the chemical pressure effect on LaNiC_2 , produced when Ni is substituted by Cu, increases the cell volume and the superconducting transition temperature from 2.7 K to about 4 K. The Cu doping affects the electronic density of states at the Fermi level $N(E_F)$ and also the electron–phonon coupling [14]. Hydrostatic and chemical pressure calculations using density functional theory explain the CDW creation and the destruction of SmNiC_2 observed in experiments [15]. These calculations are particularly in agreement with the experimental results of the effect of pressure on SmNiC_2 [13].

Chemical pressure experiments on SmNiC_2 , involving the partial substitution of one constituent element, have not yet been reported. In this work we report the chemical pressure effects on T_{CDW} and the FM transition temperature of $\text{SmNiC}_{2-x}\text{B}_x$ ($0 \leq x \leq 0.2$). The study was performed using resistance as a function of the temperature measurements. The structural analysis shows that the cell volume of $\text{SmNiC}_{2-x}\text{B}_x$ expands with boron content. As the B content increases, the CDW transition temperature decreases and depletes its intensity. The resistance as a function of temperature, above T_{CDW} , is linear and persists until the CDW vanished by the B content, suggesting a non-Fermi liquid state. Regarding the FM transition temperature, it is modified at about 5 K forming a cusp as a function of the B content. The temperature–Boron content phase diagram suggests a quantum critical behaviour.

2. Experimental details

Polycrystalline samples of $\text{SmNiC}_{2-x}\text{B}_x$ ($0 \leq x \leq 0.2$) were synthesized by arc melting in an Argon atmosphere. The samples were prepared with stoichiometric quantities of powder elements, Sm, Ni, C and B, with purities of 99.9%, 99.99%, 99.999% and 99.95%, respectively. To homogenize the samples, the obtained ingots were turned over several times, without breaking the Argon atmosphere. X-ray diffraction patterns were obtained from the powdered samples using a Siemens D-5000 diffractometer with $\text{Co-K}\alpha$ radiation ($\lambda = 1.79026 \text{ \AA}$). Measurements were obtained in the 2θ range of 20° – 95° in steps of 0.02° for 13 s, at room temperature. The structural analysis was made via the Rietveld method using the MAUD (Materials Analysis using Diffraction) program [16]. Electrical resistance measurements were carried out using a four-probe technique from room temperature down to 2 K in a PPMS (Physical Properties Measurements System) from Quantum Design.

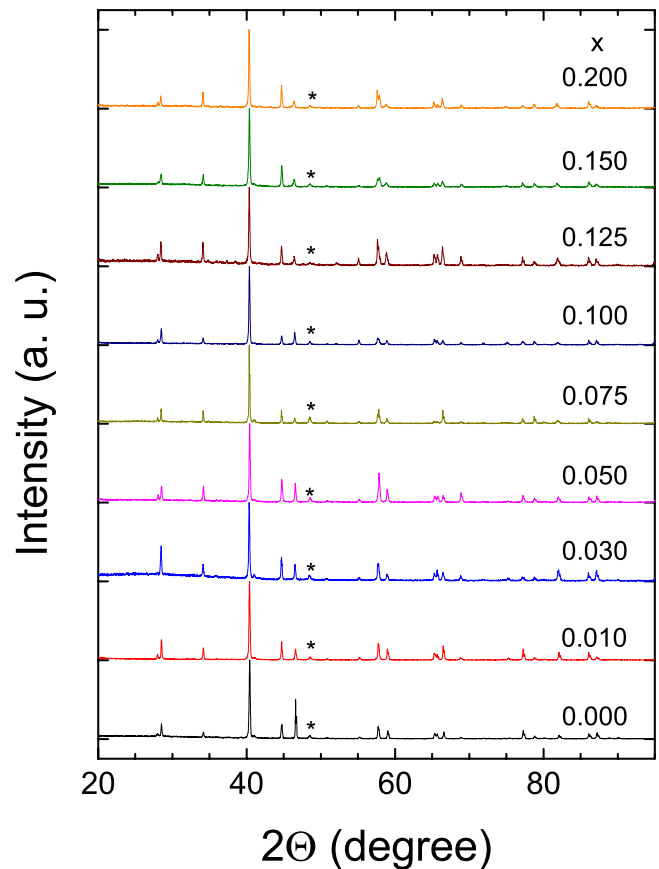


Figure 1. X-ray patterns of $\text{SmNiC}_{2-x}\text{B}_x$. The nominal content of boron is indicated. The reflections associated to Ni_2Sm impurity are indicated (*).

3. Results and discussion

X-ray patterns show the characteristic reflections of a single phase of the CeNiC_2 type, with an orthorhombic crystalline structure and space group $\text{Amm}2$. The obtained lattice parameters for SmNiC_2 were; $a = 3.7013(1) \text{ \AA}$, $b = 4.5202(1) \text{ \AA}$, and $c = 6.0911(3) \text{ \AA}$. These values are in agreement with values reported previously [1, 5, 13]. Figure 1 shows the x-ray patterns of the prepared samples. The patterns show a tiny contribution of Ni_2Sm and the reflections associated to this impurity are indicated with an asterisk. Figure 2 shows the Rietveld refinement applied to the x-ray patterns of SmNiC_2 . In this figure we plotted the experimental (dots) x-ray pattern of SmNiC_2 and the Rietveld refinement (line). The vertical lines indicate the positions of the allowed Bragg reflections of SmNiC_2 and Ni_2Sm , and at the bottom of the plot the difference between the experimental data and the Rietveld refinement is shown.

Figure 3(a) shows the change of lattice parameters $\Delta l = l_0 - l_x$, where l_0 is the lattice parameter of the sample with $x = 0$ and l_x is the lattice parameter of a sample with $x > 0$. In figure 3(b) the volume of the cell as a function of boron content is plotted. Note that the lattice parameter a has a tendency to diminish with x , meanwhile b , c and the volume increase. The biggest change in the lattice is observed in the crystal direction b .

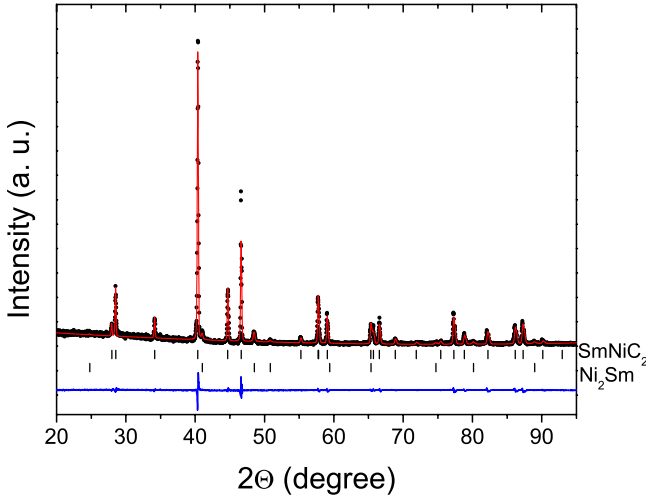


Figure 2. X-ray experimental pattern (dots) and Rietveld refinement (continuous line) of SmNiC_2 . The bars below the pattern indicate the positions of the allowed Bragg reflection of the compound and the impurity Ni_2Sm . At the bottom the difference between the experimental pattern and the Rietveld refinement is shown.

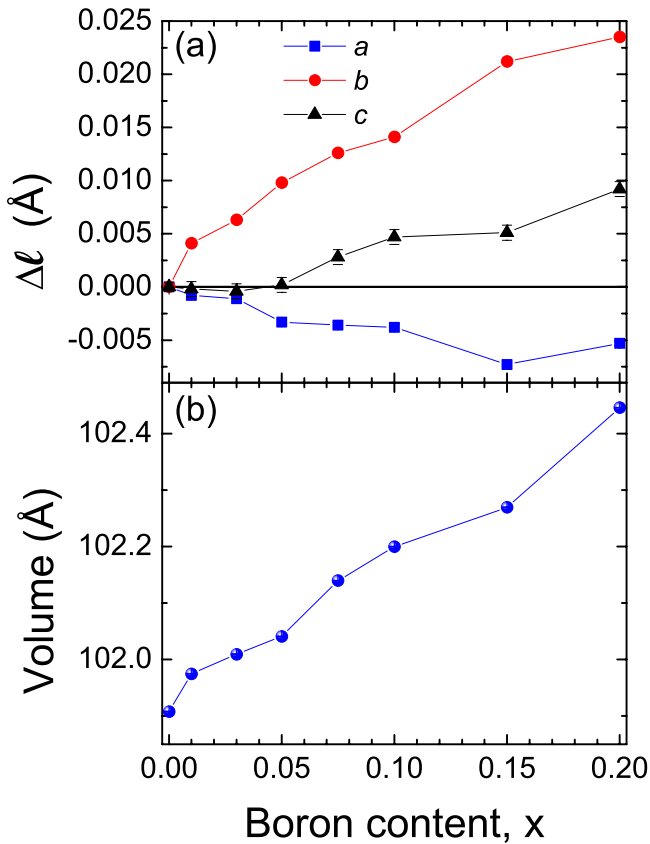


Figure 3. (a) Difference of Lattice parameters, Δl , from the value of the compound without boron ($x = 0$). (b) Volume as a function of x of $\text{SmNiC}_{2-x}\text{B}_x$.

Measurements of resistance as a function of temperature show the typical characteristic of a charge density wave. The resistance decreases from room temperature until the CDW transition temperature is reached at T_{CDW} , see figure 4. At lower temperatures the resistance increases and reaches a maximum at ~ 110 K, see the curve for $x = 0.000$. At lower temperatures, $R(T)$ again decreases until the FM transition sets

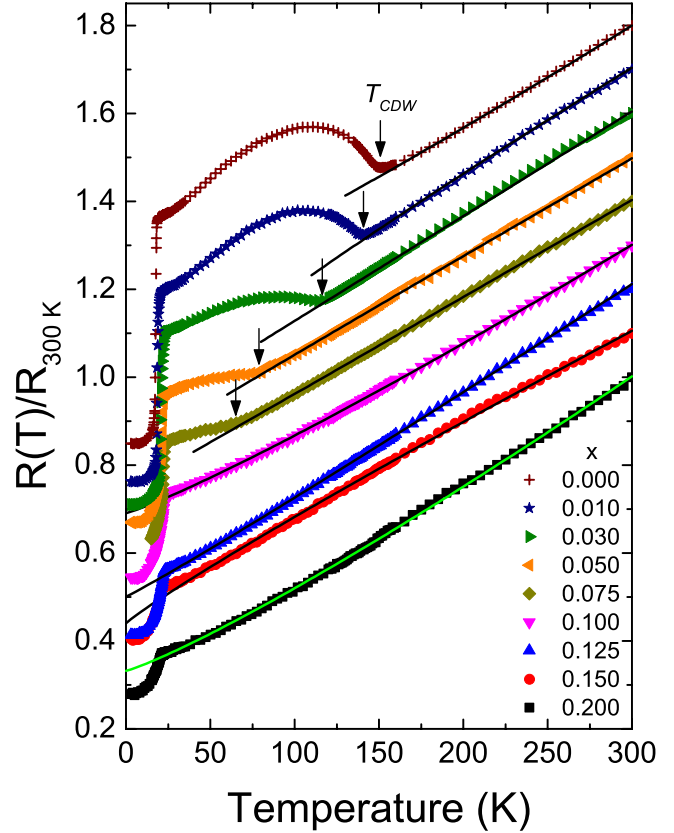


Figure 4. (Normalized resistance as a function of temperature of $\text{SmNiC}_{2-x}\text{B}_x$ ($0.000 \leq x \leq 0.200$). Curves are normalized by the resistance at 300 K and shifted vertically by clarity. The curves show the effect of boron content on the CDW, the T_{CDW} is indicated by the arrows. The continuous line is data fitting using a power law function, as discussed in the text.

at about 18 K. Following to lower temperatures the resistance decreases abruptly. When B atoms are introduced in SmNiC_2 the CDW transition temperature is clearly diminished, as depicted in figure 4. The arrows indicate the T_{CDW} . For boron content of $x = 0.100$ the T_{CDW} has vanished. We assume that the CDW disappears when boron content is between 0.075 and 0.100. Samples with $x \geq 0.100$ maintain a resistance linear behaviour from room temperature until the FM order is reached. Furthermore, the relative maximum of $R(T)$ decreases, with respect to the observed in the sample with $x = 0.000$, suggesting that the CDW is depleted with the B content. With regard to the FM state, figure 5 shows the normalized resistance, at its value at 30 K, as a function of temperature. The FM transition temperature is clearly observed as a fast decrease of the resistance, however, as the B content increases $R(T)$ decreases with a small slope. One can observe that the T_{C} increases with the B content up to when it is between $x = 0.075$ and $x = 0.100$, with a higher B content, T_{C} decreases.

The effects of the chemical pressure on the depletion and disappearance of the CDW state, as the B content increases, can be explained qualitatively from the mean field theory point of view [8, 9]. In this theory the CDW transition temperature is

$$T_{\text{CDW}} = 2.28 \frac{E_{\text{F}}}{k_{\text{B}}} e^{-\frac{1}{2N(E_{\text{F}})}} \quad (1)$$

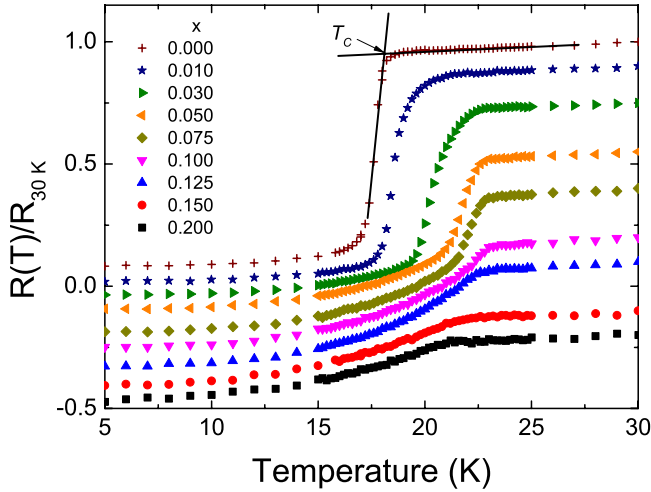


Figure 5. Normalized resistance as a function of temperature of $\text{SmNiC}_{2-x}\text{B}_x$, for x as is indicated. Curves are normalized at 30 K and show the effect of B on the FM transition temperature T_C . The curves were displaced vertically by clarity.

where k_B is the Boltzmann's constant, E_F is the Fermi energy, $N(E_F)$ is the electron density of states at the Fermi energy and g is related to the electron-phonon coupling constant. We propose that the presence of B in these compounds causes two effects; the first one is on $N(E_F)$, it is modified because of the valence difference between B and C. The second one is the difference of atomic mass between C and B, and then the phonon-modes could change. Both effects modify the electron-phonon coupling changing the conditions to form the CDW. It is easy to see from equation (1) that if g , $N(E_F)$ or both diminish then T_{CDW} decreases.

It is worth noting the linear behaviour of $R(T)$ observed above T_{CDW} in the $\text{SmNiC}_{2-x}\text{B}_x$ compounds. This behaviour persists from room temperature until the T_C when the CDW vanished for the B content $x \geq 0.100$. Linear behaviour in $R(T)$ has been observed in high temperature superconductors [17], pnictides [18–20] and other materials with strong electronic interactions [21, 22]. This behaviour can be produced by band effects and for a non-Fermi liquid state [23]. In the latter case, the resistivity as a function of temperature is linear and it has been taken as an indication for a quantum critical point (QCP) [18, 24]. The Fermi liquid is characterized by a resistivity $\rho \propto T^2$ as a result of the electron-electron interactions. However, for a non-Fermi liquid $\rho \propto T^n$, with $n \simeq 1$. In order to determine if our experimental results follow a power law at temperatures above T_{CDW} , the data were fitted with $R(T) = A + BT^\alpha$, where A and B are constants. The α values obtained from the fitting are around 1, but these values do not have a trend with the boron content. The sample with $x = 0.200$ has the higher value, $\alpha = 1.157 \pm 0.007$. Taking in account the α values of all samples, the mean value is $\bar{\alpha} = 0.98 \pm 0.14$. It is well known that a linear behaviour is produced by the electron-phonon interaction at temperatures between the Debye temperature Θ_D and the Fermi temperature T_F [24]. The Debye temperature reported for SmNiC_2 is 275 K, obtained from nuclear resonant inelastic scattering (NRIS) experiments in an indirect way

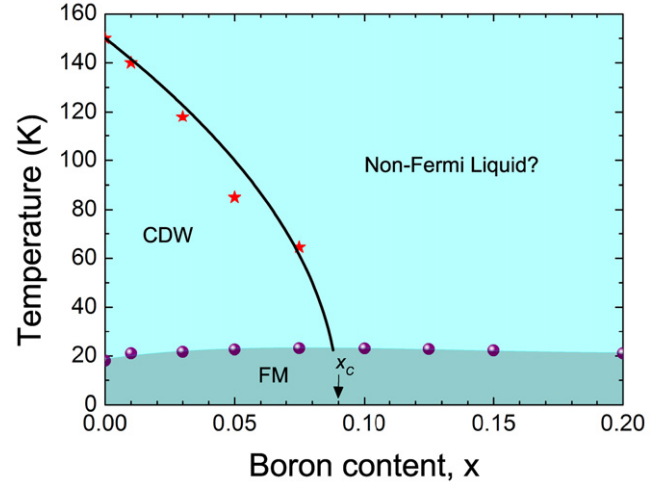


Figure 6. Phase diagram Temperature-Boron content of $\text{SmNiC}_{2-x}\text{B}_x$. The stars represent the CDW transition temperature and the dots are the ferromagnetic transition temperatures. The thick line is a data fit using a mean field power law and x_c is the critical boron content, $x_c = 0.090$.

[25]. This value is lower than the values obtained from heat capacity experiments in isostructural compounds. For $(\text{Dy}, \text{Ho}, \text{Er})\text{NiC}_2$ and YNiC_2 compounds $\theta_D = 381$ K and $\theta_D = 456$ K were reported, respectively [26]. The values obtained from heat capacity experiments are more reliable than those obtained from NRIS experiments. The temperature range where $\text{SmNiC}_{2-x}\text{B}_x$ compounds show a linear behaviour of $R(T)$ is well below the region where electron-phonon dispersion produces a linear behaviour on resistivity. The fact that $\text{SmNiC}_{2-x}\text{B}_x$ compounds show a linear behaviour of $R(T)$, down to the FM order temperature, suggests that the electronic behaviour could be due to a non-Fermi liquid, and that the system is close to a QCP.

The chemical pressure effects, produced when C is substituted by B, on the CDW transition temperature and on the FM transition temperature is summarized in figure 6. This figure represents the temperature-boron content phase diagram. The diagram shows that the effect on T_C is modest in the studied C substituted range. The maximum change of T_C is about 5 K, from $T_C \simeq 18$ K ($x = 0.000$) to $T_C \simeq 23.1$ K ($x = 0.075$). With regard to the T_{CDW} , it is depleted rapidly with the B content, from 150 K ($x = 0.000$) to ~ 64.5 K ($x = 0.075$). In this figure the T_{CDW} experimental values are represented by stars and the continuous line that delimits the CDW region is the best fit of $T_{\text{CDW}}(x)$. The fitting was obtained with a mean field power law function of the type often used to describe the $T_{\text{CDW}} - \text{Pressure}$ behaviour [11]. The charge density wave transition temperature is

$$T_{\text{CDW}}(x) = T_{\text{CDW}}(0) \sqrt{1 - \frac{x}{x_c}},$$

where $T_{\text{CDW}}(0)$ is the CDW transition temperature for the sample with $x = 0.000$, and x_c is the B content that corresponds to $T_{\text{CDW}} = 0$ K, in this case the critical B content $x_c \simeq 0.090$, however, it is known that the CDW disappears when the temperature reaches T_C [6]. The point where the three states coexist is at $x \simeq 0.088$ and $T \simeq 23$ K.

Assuming that the region above the FM state and to the right of the CDW state is a non-Fermi liquid state, the phase diagram suggests the existence of a quantum critical point. However, to confirm this assumption, further experiments will be performed in order to demonstrate unambiguously the non-Fermi liquid state.

4. Conclusions

We have investigated the effects of C substituted by B on a SmNiC₂ compound. The structural changes observed indicate a chemical pressure effect produced by the substitution of C by B. This structural modification causes T_{CDW} to diminish with an increment of boron content following a mean field power law. Meanwhile the T_C as a function of B content shows a tiny dome. The temperature-boron content phase-diagram, assuming a non-Fermi liquid state, suggests the presence of a quantum critical behaviour.

Acknowledgments

The authors thank R Escudero for helpful discussions, and D Mendoza and E Geffroy for their critical reading of the manuscript. We acknowledge F Silvar for providing technical support.

References

- [1] Onodera H, Koshikawa Y, Kosaka M, Ohashi M, Yamauchi H and Yamaguchi Y 1998 *J. Magn. Magn. Mater.* **182** 161–71
- [2] Yamamoto N, Kondo R, Maeda H and Nogami Y 2013 *J. Phys. Soc. Japan* **82** 123701
- [3] Lee W H, Zenf H K, Yao Y D and Chen Y Y 1996 *Physica C* **266** 138–42
- [4] Pecharsky V K, Miller L L and Gschneidner J K A 1998 *Phys. Rev. B* **58** 497
- [5] Wölfel A, Li L, Shimomura S, Onodera H and van Smaalen S 2010 *Phys. Rev. B* **82** 054120
- [6] Shimomura S, Hayashi C, Asaka G, Wakabayashi N, Mizumaki M and Onodera H 2009 *Phys. Rev. Lett.* **102** 076404
- [7] Briggs A, Monceau P, Nunez-Regueiro M, Peyrard J, Ribault M and Richard J 1980 *J. Phys. C: Solid State Phys.* **13** 2117
- [8] Grüner G 1994 *Density Waves in Solids (Frontiers in Physics vol 89)* (New York: Addison-Wesley)
- [9] Monceau P 2012 *Adv. Phys.* **61** 325–581
- [10] Badding J V 1998 *Annu. Rev. Mater. Sci.* **28** 631–58
- [11] Monteverde M, Lorenzana J, Monceau P and Núñez Regueiro M 2013 *Phys. Rev. B* **88** 180504
- [12] Kiswandhi A, Brooks J S, Lu J, Whalen J, Siegrist T and Zhou H D 2011 *Phys. Rev. B* **84** 205138
- [13] Woo B, Seo S, Park E, Kim J H, Jang D, Park T, Lee H, Ronning F, Thompson J D, Sidorov V A and Kwon Y S 2013 *Phys. Rev. B* **87** 125121
- [14] Sung H H, Chou S Y, Syu K J and Lee W H 2008 *J. Phys.: Condens. Matter* **20** 165207
- [15] Kim J N, Lee C and Shim J H 2013 *New J. Phys.* **15** 123018
- [16] Lutterotti L and Gialanella S 1998 *Acta Mater.* **46** 101
- [17] Ando Y, Komiya S, Segawa K, Ono S and Kurita Y 2004 *Phys. Rev. Lett.* **93** 267001
- [18] Gooch M, Bing L v, Lorenz B, Guloy A M and Chu C W 2009 *Phys. Rev. B* **79** 104504
- [19] Kasahara S *et al* 2010 *Phys. Rev. B* **81** 184519
- [20] Analytis J G, Kuo H H, McDonald R D, Wartenbe M, Rourke P M C, Hussey N E and Fisher I R 2014 *Nat. Phys.* **10** 194
- [21] Vescoli V, Degiorgi L, Henderson W, Grüner G, Starkey K P and Montgomery L K 1998 *Science* **281** 1181
- [22] Morosan E, Zandbergen H W, Dennis B S, Bos J W G, Onose Y, Klimczuk T, Ramirez A P, Ong N P and Cava R J 2006 *Nat. Phys.* **2** 544
- [23] Varma C M, Nussinov Z and Saarloos W 2002 *Phys. Rep.* **361** 267–417
- [24] Löhneysen H V, Rosch A, Vojta M and Wölfle P 2007 *Rev. Mod. Phys.* **79** 1013
- [25] Tsutsui S, Shimomura S, Yoda Y, Kobayashi H and Onodera H 2014 *Hyperfine Interact.* **226** 637
- [26] Long Y, Zheng C Z, Luo J L, Cheng Z J and He Y S 2001 *J. Appl. Phys.* **89** 3523